Absorptivity of Functionalized Single-Walled Carbon Nanotubes in Solution

Bing Zhou,[†] Yi Lin,[†] Huaping Li,[†] Weijie Huang,[†] John W. Connell,[‡] Lawrence F. Allard,[§] and Ya-Ping Sun*,[†]

Department of Chemistry, Howard L. Hunter Chemistry Laboratory, Clemson University, Clemson, South Carolina 29634-0973, Advanced Materials and Processing Branch, NASA Langley Research Center, Mail Stop 226, Hampton, Virginia 23681-2199, and High-Temperature Materials Laboratory, Oak Ridge National Laboratory, Oak Ridge, Tennessee 37831-6062

Received: June 10, 2003; In Final Form: September 2, 2003

Single-walled carbon nanotubes (SWNTs) were solubilized by attaching functional groups to the nanotube-bound carboxylic acids in the esterification and various amidation reactions. The solubility made it possible to not only characterize the functionalized SWNT samples in solution but also quantitatively measure the UV/vis/NIR absorption spectra of the samples. The nanotube contents in the soluble samples were determined in terms of NMR signal integrations in reference to internal standards and through thermal gravimetric analyses. The absorptivity results thus obtained are similar for SWNTs in the different functionalized samples. For the near-infrared absorption band corresponding to the first pair of van Hove singularities in the electronic density of states for semiconducting SWNTs, the peak absorptivity is 0.5−2.2 $(mg/mL)^{-1}$ cm^{-1}. The absorption properties of SWNTs are apparently insensitive to changes in the sample environment, such as the functionalization with significantly different groups. The effects of scattering on the accurate determination of absorptivity are discussed.

Introduction

Carbon nanotubes are colored species, with light absorption due to electronic transitions extending well into the near-infrared (NIR) region.[1−7] In fact, NIR absorption spectroscopy has become a valuable technique for the characterization of carbon nanotubes.[3−7] For example, Haddon and co-workers reported recently on the use of NIR spectroscopy to evaluate the purity of as-prepared single-walled carbon nanotube (SWNT) soot.[5] However, there has not been much effort on determining the absorptivity of carbon nanotubes, which may be due to the general insolubility of carbon nanotubes. Absorption measurements of suspended carbon nanotubes in organic solvents and water are often subject to substantial interference from the scattering of light by the nanotube bundles. Thus, solubilized carbon nanotubes in homogeneous solution are required to begin a quantitative evaluation of the absorption parameters.

The solubilization of SWNTs has been achieved via functionaliztion reactions in two categories. One includes chemical reactions for direct addition to the nanotube graphitic walls,[8−10] and the other involves functionalization via the attachment of oligomeric or polymeric species at the nanotube defect sites.[11−19] The latter typically involves the nanotube-bound carboxylic acids, which allow the formation of ionic, ester, or amide linkages with various functionalities. The functionalization via reactions with the nanotube-bound carboxylic acids should in principle preserve the electronic structures and thus absorption properties of SWNTs, though effects of noncovalent interactions between the nanotube and functional groups and other potential damages to the nanotube as a result of the functionalization reactions remain popular subjects of investigation by the research community. Nevertheless, the solubilization allows not only the homogeneous dispersion but also an accurate determination of the concentration of SWNTs, both of which are required for the absorptivity evaluation.

In this paper, we report a determination of the absorptivity of functionalized SWNTs. The functionalization was based on various reactions of the diamine-terminated oligomeric poly(ethylene glycol) and the dendron 3,5-(dihexadecoxy)benzyl alcohol with the nanotube-bound carboxylic acids, rendering the solubility necessary for the formation of homogeneous solutions. In addition to the characterization of the functionalized SWNTs, the nanotube contents in the soluble samples were determined by using both solution-phase and solid-state techniques. The absorptivity values thus obtained are discussed in reference to what are available in the literature.

Experimental Section

Materials. Diamine-terminated oligomeric poly(ethylene glycol), $H_2NCH_2CH_2CH_2(OCH_2CH_2)_nCH_2NH_2$, with $n \sim 35$ (PEG_{1500N}) was purchased from Aldrich and used after removing the residual water via azeotropic distillation. 1-Ethyl-3-[3-(dimethylamino)propyl]carbodiimide hydrochloride (EDAC, 98+%) was obtained from Alfa Aesar. Thionyl chloride (99.5+%) was provided by Acros. All solvents were either of spectrophotometry/HPLC grade or purified via simple distillation. Deuterated solvents for NMR measurements were supplied by Cambridge Isotope Laboratories. Dialysis tubing made of cellulose ester membrane was obtained from Spectrum Laboratory Products.

The SWNT sample was produced in Prof. A. M. Rao's laboratory (Physics Department, Clemson University) by using the arc-discharge method with Ni/Y as catalyst. In the purification to remove catalyst particles, the SWNT sample was heated and stirred in aqueous HNO_3 solution (2.6 M) for 48 h. Upon

[†] Clemson University.
[‡] NASA Langley Research Center.
[§] Oak Ridge National Laboratory.

10.1021/jp0307248 CCC: $25.00
Published on Web 11/14/2003

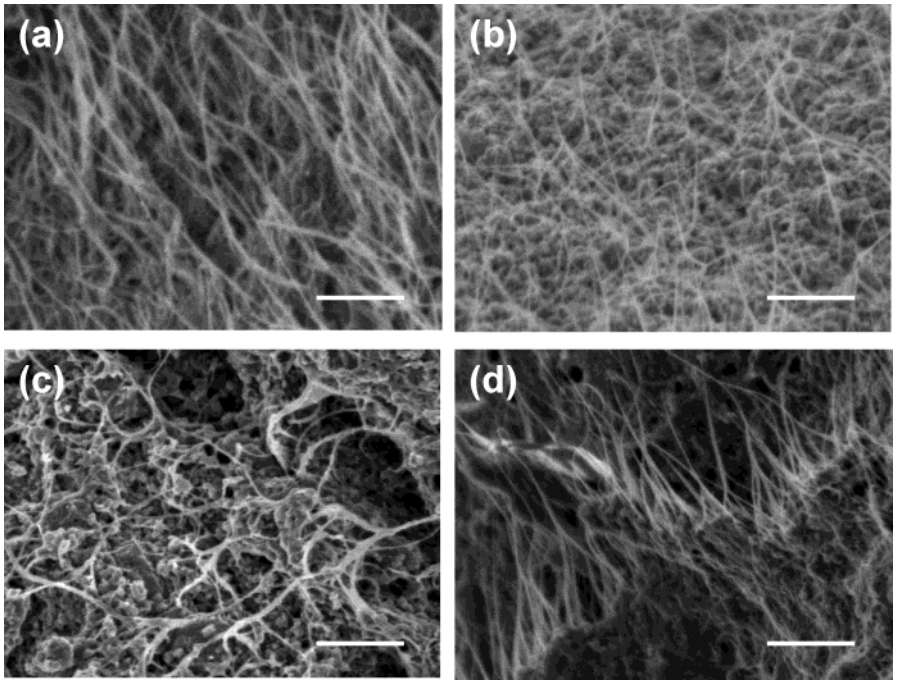

Figure 1. SEM images of (a) the purified SWNT sample and the PEG_{1500N}-SWNT samples obtained from (b) thermal reaction, (c) acylation−amidation, and (d) EDAC-activated coupling. The functionalized samples were thermally defunctionalized before SEM imaging. All scale bars represent 400 nm.

centrifuging, the solid sample was recovered, washed repeatedly with deionized water, and then suspended in water with the surfactant Triton X-100. The aqueous suspension was passed through a 200 nm membrane cartridge in a cross-flow filtration system (Spectrum MiniKros Lab).[20] After an elaborate washing process to remove the surfactant, the final purified SWNT sample was obtained. A scanning electron microscopy (SEM) image of the sample is shown in Figure 1.

Measurement. UV/vis/NIR absorption spectra were recorded on a Shimadzu UV3100 spectrophotometer and a Thermo-Nicolet Nexus 670 FT-NIR spectrometer. Raman spectra were obtained on a Renishaw Raman spectrometer equipped with a 50 mW diode laser source for 780 nm excitation and a CCD detector. NMR measurements were carried out on a JEOL Eclipse +500 NMR spectrometer. Thermal gravimetric analysis (TGA) was performed on a Mettler-Toledo TGA/SDTA851e system. SEM images were obtained on a Hitachi S4700 field-emission SEM system. Transmission electron microscopy (TEM) analyses were conducted on a Hitachi HF-2000 TEM system equipped with a Gatan Multiscan CCD camera for digital imaging.

Functionalization Reactions. SWNTs were functionalized with PEG_{1500N} in three different reactions: direct thermal reaction, acylation−amidation, and carbodiimide-activated coupling.

In the thermal reaction, a purified SWNT sample (22 mg) was mixed with PEG_{1500N} (415 mg) and stirred at ∼140 °C for 24 h. The reaction mixture was dispersed into deionized water for dialysis (cutoff molecular weight of the dialysis tubing ∼12 000) against fresh deionized water for 3 days. Upon vigorous centrifuging (∼3100 g) to recover insoluble nanotubes, a dark-colored solution of the PEG_{1500N}-functionalized SWNTs was obtained.

In the acylation−amidation reaction, a purified SWNT sample (25 mg) was refluxed in $SOCl_2$ for 24 h to convert the nanotube-bound carboxylic acids into acyl chlorides.[5] After a complete removal of residual $SOCl_2$ on a rotary evaporator with a vacuum pump, the sample was mixed well with the carefully dried PEG_{1500N} (420 mg) in a flask, heated to ∼140 °C, and vigorously stirred for 24 h under a nitrogen atmosphere. The same dialysis process as described above, followed by vigorous centrifuging, also yielded a dark-colored solution of the PEG_{1500N}-functionalized SWNTs.

In the reaction of amidation via EDAC-activated coupling, a purified SWNT sample (30 mg) was suspended in aqueous KH_2PO_4 buffer (pH = 6−7, 25 mL). To the suspension was added PEG_{1500N} (300 mg) and EDAC (112 mg, 60 mmol). After sonication (power ∼ 30 W) at room temperature for 24 h, the same dialysis and centrifuging processes as described above were applied to obtain a dark-colored solution of the PEG_{1500N}-functionalized SWNTs.

The synthesis and characterization of **I**-SWNT have been reported in detail previously.[15a]

Results and Discussion

The PEG_{1500N}-functionalized SWNTs are soluble in more polar solvents such as THF and chloroform and in water, forming dark-colored homogeneous solutions. On the other hand, the **I**-SWNT sample is soluble in CS_2 and ether, but obviously not in water. The solubilities of these functionalized carbon nanotube samples in various solvents make it possible to carry out both the characterization and the study of fundamental properties in solution.

Sample Characterization. The solution-phase ^1H NMR spectra of the PEG_{1500N}-functionalized SWNT samples obtained in three different reactions are compared with that of the neat PEG_{1500N} in Figure 2. All three spectra of the functionalized nanotube samples are characterized by a signal at ∼3.65 ppm, which are broader than the same signal of neat PEG_{1500N}. The broadening is likely a result of the PEG_{1500N} oligomers being attached to the nanotubes as large species of a low mobility.[15a,16]

The solutions of the functionalized carbon nanotube samples allow the deposition of the samples onto TEM grids without significantly altering the dispersion of the nanotubes. However,

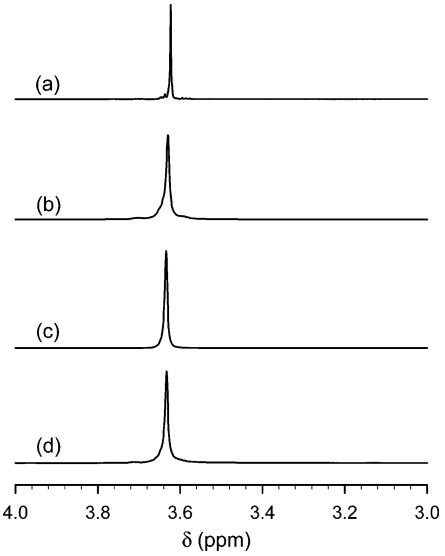

Figure 2. ^{1}H NMR spectra of (a) PEG_{1500N} and the PEG_{1500N}-SWNT samples obtained from (b) thermal reaction, (c) acylation−amidation, and (d) EDAC-activated coupling.

the TEM imaging of functionalized SWNTs is intrinsically difficult because of a lack of contrast due to the presence of a large amount of functional groups. Thus, a specifically designed $LaCrO_3$-coated holey stainless steel grid was used to allow ex situ thermal treatment of the specimen on the grid to partially remove the functional groups.[13] The TEM images thus obtained show that the nanotubes are well dispersed in the PEG_{1500N}-SWNT samples.

The removal or partial removal of functional groups is also required for the Raman characterization of the functionalized SWNTs to eliminate or reduce the overwhelming luminescence interference.[13] Thermal defunctionalization of the functionalized SWNTs in slow TGA scans represents an effective method for such a purpose. As compared in Figure 1, the SEM images of the PEG_{1500N}-functionalized SWNT samples after thermal defunctionalization are similar to that of the purified SWNT sample. The same thermally defunctionalized PEG_{1500N}-SWNT samples were measured by Raman spectroscopy. The spectra show the characteristic Raman peaks of SWNTs, including the radial breathing mode signals in the low-frequency region (Figure 3).

Absorption and Absorptivity. The UV/vis/NIR absorption spectra of the PEG_{1500N}-SWNT samples obtained from three different functionalization reactions and the **I**-SWNT sample were measured in homogeneous solutions (Figure 4). Because the functional groups (PEG_{1500N} and dendron **I**) and the solvents have no absorption contributions in the UV (300−400 nm) and visible wavelength regions, the absorption spectra of the functionalized SWNTs were obtained without substantial background corrections. In the NIR region, however, the solvents in which the PEG_{1500N}-SWNT samples are soluble all have strong absorption peaks, making it impossible to determine the sample absorptions at those wavelengths. Thus, the NIR spectra of the PEG_{1500N}-SWNT samples were measured in the solid state (a thin film obtained by depositing the sample solution onto a glass slide and then evaporating the solvent, Figure 4d). For **I**-SWNT, which is soluble in CS_2, the solvent background in the NIR region is relatively weak. The NIR absorptions of the sample were determined in both CS_2 solution and the solid state. The spectra thus obtained are rather similar, as compared in Figure 4, suggesting that the NIR absorptions of the functionalized SWNTs are insensitive to the medium conditions. Because

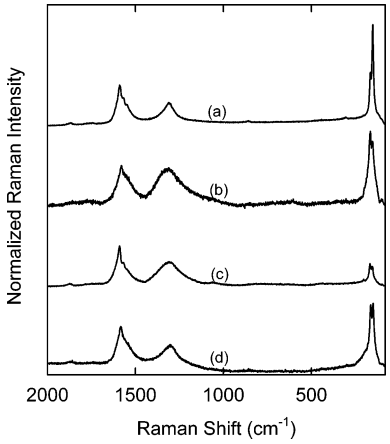

Figure 3. Raman spectra of (a) the purified SWNT sample and the PEG_{1500N}-SWNT samples obtained from (b) thermal reaction, (c) acylation−amidation, and (d) EDAC-activated coupling. The functionalized samples were thermally defunctionalized before the Raman measurements.

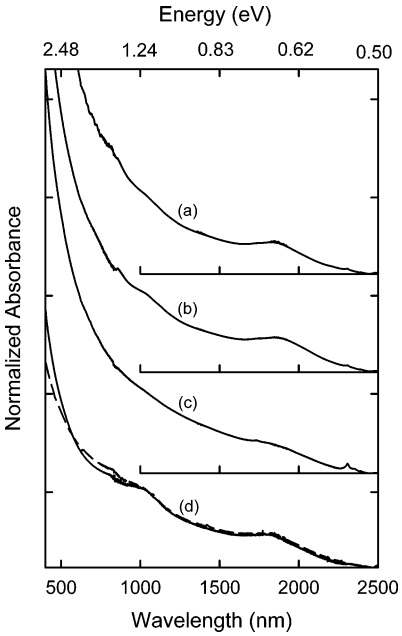

Figure 4. Absorption spectra of the PEG_{1500N}-SWNT samples obtained from (a) thermal reaction, (b) acylation−amidation, and (c) EDAC-activated coupling compared with those of (d) **I**-SWNT in a solid-state film (—) and in CS_2 solution (− − −).

the optical path length is more accurately defined in the solution-phase measurement, the NIR absorptions of the PEG_{1500N}-SWNT samples were also determined at some selected wavelengths. The results were used to scale the spectra obtained in the solid state to the correct optical path length for subsequent absorptivity calculations.

The observed absorption spectra after the correction for solvent background are still affacted by the light scattering due to the large sizes of the absorbing species. In fact, an accurate determination of the scattering contributions is very difficult. In this study, we rely on two extreme assumptions. One extreme is that the scattering contributions are wavelength independent, which can thus be offset (made to zero) at 2500 nmm as in Figure 4. The absorptivity values calculated from the resulting spectra might be considered as being at the upper limit (Figure 5).

The assumption at the other extreme is that the NIR absorption bands of the functionalized SWNTs are discrete

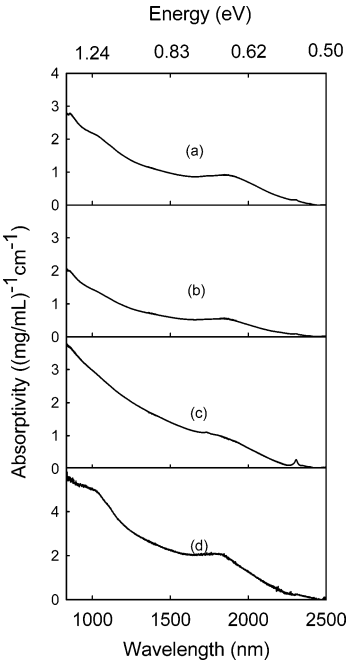

Figure 5. Absorptivity results of the PEG_{1500N}-SWNT samples obtained from (a) thermal reaction, (b) acylation−amidation, and (c) EDAC-activated coupling compared with those of (d) **I**-SWNT.

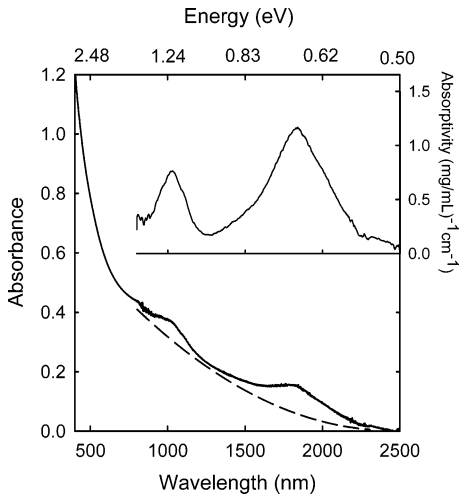

Figure 6. NIR absorptions of **I**-SWNT estimated by subtracting a curved scattering background (− − −) from the observed absorption spectrum.

peaks. A common practice in the literature has been to assign absorptions in the NIR region to the transitions associated with the first and second pairs of van Hove singularities in the electronic density of states for semiconducting SWNTs.[1−7] Under the assumption, a curve was generated in such a way that when it was subtracted from the observed spectrum, the two discrete absorption bands similar to those already reported in the literature could be obtained (Figure 6). The absorptivity values calculated from the resulting NIR absorption spectrum should be at the lower limit (Figure 6, inset).

An accurate determination of the nanotube contents in the functionalized SWNT samples (containing SWNTs and the functional groups) was required for the absorptivity calculations. Quantitative ^{1}H NMR and TGA measurements of the samples in solution and the solid state, respectively, were used for such a purpose. In the quantitative ^{1}H NMR analysis, several internal ^{1}H standards including acetone, acetonitrile, dimethyl sulfoxide, and chloroform were employed. The internal standards were

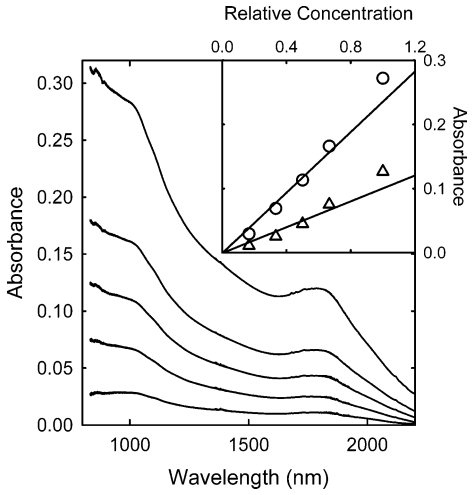

Figure 7. Concentration dependence of the **I**-SWNT NIR absorptions. Shown in the inset are plots for the results at the S_{11} (1842 nm, △) and S_{22} (1037 nm, ○) peaks.

TABLE 1: Nanotube Contents in the Functionalized SWNT Samples

		nanotube content, wt %	
sample	functionalization reaction	TGA	NMR
PEG_{1500N}-SWNT	thermal reaction	20	23
PEG_{1500N}-SWNT	acylation−amidation	12	17
PEG_{1500N}-SWNT	EDAC-activated amidation	16	11
I-SWNT	acylation−amidation	40	36

calibrated against one another for consistency. The results thus obtained for the functionalized SWNT samples are shown in Table 1. Separately, the same samples in the solid state were measured quantitatively by TGA to determine the SWNT contents. The results are compared with those from the NMR analysis in Table 1. Despite the fact that all these measurements allow only rough estimates, the SWNT contents obtained from the two different methods are in reasonable agreement.

The absorptivity values were calculated from the absorption spectra in Figure 4 and the nanotube content results in Table 1 for SWNTs in the functionalized samples (Figure 5). As compared in Table 2, the results for different functionalized SWNT samples are similar in the sense that they are all within the same order of magnitude. This is interesting because the nanotubes are functionalized with groups of significantly different properties. Additionally, the nanotube dispersion in the PEG_{1500N}-SWNT samples from different functionalization reactions is likely different, with the EDAC-activated amidation typically yielding more functionalized nanotube bundles.[13] Such effects apparently cause no dramatic changes to the observed absorptivity of SWNTs in the functionalized samples.

The solution concentration dependence of the observed absorbance follows the Lambert−Beer's law at low SWNT concentrations and slightly deviates upward at higher SWNT concentrations (Figure 7). The upward deviation might be a result of light scattering contributions. Even the apparently linear relationship at low concentrations does not necessarily exclude the possibility for contributions from light scattering in the observed absorption spectra. As discussed above, the absorptivity values obtained from the spectra in Figure 4 and Figure 7 are likely at the upper limit. The lower limit is shown in Figure 6. Thus, the absorptivity of **I**-SWNT at the peak for transition corresponding to the first pair of van Hove singularities in the electronic density of states for semiconducting SWNTs (S_{11}) is 1.2−2.2 (mg/mL)$^{-1}$cm^{-1}. As a reference, fullerene C_{60} has a

TABLE 2: Absorptivity of SWNTs in the Functionalized Samples[a]

sample	functionalization reaction	absorptivity, $(mg/mL)^{-1}$ cm^{-1}		
		500 nm	S_{22}[b]	S_{11}[c]
PEG_{1500N}-SWNT	thermal reaction	5.92	0.9	
PEG_{1500N}-SWNT	acylation−amidation	4.6	1.3	0.5
PEG_{1500N}-SWNT	EDAC-activated amidation	9.3	2.8	0.8
I-SWNT	acylation−amidation	9.7	4.9 (0.76)[d]	2.2 (1.2)[d]
average (standard deviation):		7.4 (2.5)	2.8 (1.5)	1.1 (0.8)

[a] The average of the SWNT contents from the two methods in Table 1 used in the calculation. An implicit assumption in the absorptivity calculation is the same absorptivity for every nanotube carbon, regardless of the nanotube size and other properties. [b] 1052 nm, except for I-SWNT at 1037 nm. [c] 1880 nm, except for I-SWNT at 1840 nm. [d] From the inset of Figure 6.

peak absorptivity in the visible (540 nm) of 1.3 $(mg/mL)^{-1}$ cm^{-1}.[21] Because C_{60} is often considered a very weak visible absorber, SWNTs are still weak absorbers in the visible and near-IR regions.

The absorptivity is an important parameter for carbon nanotubes. However, reports on the relevant investigations have been scarce at best.[22,23] Bahr et al. reported that the SWNTs from the HiPco process could be well suspended in 1,2-dichlorobenzene, with the observed absorptivity at 500 nm of 28.6 $(mg/mL)^{-1}$ cm^{-1}.[23] The absorptivity value was then used to determine the concentrations or solubilities of the HiPco-SWNTs in other organic solvents.[23] The scattering contribution could be a factor for the larger absorptivity of the HiPco-SWNT sample than those determined here, though it should also be recognized that the SWNT samples produced by the different methods could have different absorption properties. An even larger absorptivity value at 500 nm was estimated in the study of chemical defunctionalization of functionalized SWNTs, where the amount of nanotubes recovered from the defunctionalization reaction was correlated with the decrease in the absorption of the nanotube solution.[15b] However, the result was probably subject to significant scattering effects because the relatively larger SWNT bundles, corresponding to stronger scatters, were likely precipitated first in the chemical defunctionalization reaction, resulting in an overestimation of the absorptivity.

The absorptivity values reported here are obviously rough averages because SWNTs of different lengths and diameters may have different per-unit-weight absorptivities. The functionalization reactions may also be selective with respect to some nanotube parameters (such as the diameter[24,25]), which presents additional challenges to the study of nanotube absorptivity. Further investigations are required for an improved understanding and a more accurate determination of the absorptivities of different carbon nanotubes under various experimental conditions.

Acknowledgment. We thank Prof. A. M. Rao for supplying the carbon nanotube samples and S. Fernando for experimental assistance. Financial support from NSF, NASA, and the Center for Advanced Engineering Fibers and Films (NSF-ERC at Clemson University) is gratefully acknowledged. Research at Oak Ridge National Laboratory was sponsored by the Assistant Secretary for Energy Efficiency and Renewable Energy, Office of Transportation Technologies, as part of the HTML User Program, managed by UT-Battelle LLC for U.S. DOE under contract number DE-AC05-00OR22725.

References and Notes

(1) (a) Wilder J. W. G.; Benena, L. C.; Rinzler, A. G.; Smalley, R. E.; Dekker, C. *Nature* **1998**, *391*, 59. (b) Pichler, T.; Knupfer, M.; Golden, M. S.; Fink, J.; Rinzler A.; Smalley R. E. *Phys. Rev. Lett.* **1998**, *80*, 4729.

(2) Odom, T. W.; Huang, J.-L.; Kim, P.; Lieber, C. H. *Nature* **1998**, *391*, 62.

(3) Hamon, M. A.; Itkis, M. E.; Niyogi, S.; Alvaraez, T.; Kuper, C.; Menon, M.; Haddon, R. C. *J. Am. Chem. Soc.* **2001**, *123*, 11292.

(4) Itkis, M. E.; Niyogi, S.; Meng, M.; Hamon, M.; Hum H.; Haddon, R. C. *Nano Lett.* **2002**, *2*, 155.

(5) Itkis, M. E.; Perea, D. E.; Niyogi, S. M.; Rickard, S. M.; Hamon, M. A.; Hu, H.; Zhao, B.; Haddon, R. C. *Nano Lett.* **2003**, *3*, 309.

(6) Kukovecz, A.; Kramberger, Ch.; Holzinger, M.; Kuzmany, H.; Schalko, J.; Mannsberger, M.; Hirsch, A. *J. Phys. Chem. B.* **2002**, *106*, 6374.

(7) (a) Chiang, I. W.; Brinson, B. E.; Smalley, R. E.; Margrave, J. L.; Hauge, R. H. *J. Phys. Chem. B* **2001**, *105*, 1157. (b) Chiang, I. W.; Brinson, B. E.; Huang, A. Y.; Willis, P. A.; Bronikowskim M. J.; Margrave, J. L.; Smalley, R. E.; Hauge, R. H. *J. Phys. Chem. B* **2001**, *105*, 8297.

(8) Khabashesku, V. N.; Billups, W. E.; Margrave, J. L. *Acc. Chem. Res.* **2002**, *35*, 1087.

(9) Bahr, J. L.; Tour, J. M. *J. Mater. Chem.* **2002**, *12*, 1952.

(10) Hirsch, A. *Angew. Chem., Int. Ed.* **2002**, *41*, 1853.

(11) Chen, J.; Hamon, M. A.; Hu, H.; Chen, Y.; Rao, A. M.; Eklund, P. C.; Haddon, R. C. *Science* **1998**, *282*, 95.

(12) Niyogi, S.; Hamon, M. A.; Hu, H.; Zhao, B.; Bhowmik, P.; Sen, R.; Itkis, M. E.; Haddon, R. C. *Acc. Chem. Res.* **2002**, *35*, 1105.

(13) Sun, Y.-P.; Fu, K.; Lin, Y.; Huang, W. *Acc. Chem. Res.* **2002**, *35*, 1096.

(14) Chen, J.; Rao, A. M.; Lyuksyutov, S.; Itkis, M. E.; Hamon, M. A.; Hu, H.; Cohn, R. W.; Eklund, P. C.; Colbert, D. T.; Smalley, R. E.; Haddon, R. C. *J. Phys. Chem. B* **2001**, *105*, 2525.

(15) (a) Sun, Y.-P.; Huang, W.; Lin, Y.; Fu, K.; Kitaygorodskiy, A.; Riddle, L. A.; Yu, Y. J.; Carroll, D. L. *Chem. Mater.* **2001**, *13*, 2864. (b) Fu, K.; Huang, W.; Lin, Y.; Riddle, L. A.; Carroll, D. L.; Sun, Y.-P. *Nano Lett.* **2001**, *1*, 439.

(16) Huang, W.; Fernando, S.; Allard, L. F.; Sun, Y.-P. *Nano Lett.* **2003**, *3*, 565.

(17) (a) Jin, Z.; Sun, X.; Xu, G.; Goh, S. H.; Ji, W. *Chem. Phys. Lett.* **2000**, *318*, 505. (b) Sano, M.; Kamino, A.; Okamura, J.; Shinkai, S. *Langmuir* **2001**, *17*, 5125.

(18) Pompeo, F.; Resasco, D. E. *Nano Lett.* **2002**, *2*, 369.

(19) Banerjee, S.; Wong, S. S. *J. Am. Chem. Soc.* **2002**, *124*, 8940.

(20) Liu, J.; Rinzler, A. G.; Dai, H. J.; Hafner, J. H.; Bradley, R. K.; Boul, P. J.; Lu, A.; Iverson, T.; Shelimov, K.; Huffman, C. B.; Rodriguez-Macias, F.; Shon, Y. S.; Lee, T. R.; Colbert, D. T.; Smalley, R. E. *Science* **1998**, *280*, 1253.

(21) (a) Sun, Y.-P.; Wang, P.; Hamilton, N. B. *J. Am. Chem. Soc.* **1993**, *115*, 6378. (b) Sun, Y.-P. In *Molecular and Supramolecular Photochemistry*; Ramamurthy, V., Schanze, K. S., Eds.; Marcel Dekker: New York, 1997; Vol. 1, p 325.

(22) Ausman, K. D.; Piner, R.; Lourie, O.; Ruoff, R. S.; Korobov, M. *J. Phys. Chem. B* **2000**, *104*, 8911.

(23) Bahr, J. L.; Mickelson, E. T.; Bronikowski, M. J.; Smalley, R. E.; Tour, J. M. *Chem. Commun.* **2001**, 193.

(24) Georgakilas, V.; Voulgaris, D.; Vazquez, E.; Prato, M.; Guldi, D. M.; Kukovecz, A.; Kuzmany, H. *J. Am. Chem. Soc.* **2002**, *124*, 14318.

(25) Huang, W.; Fernando, S.; Lin, Y.; Zhou, B.; Allard, L. F.; Sun, Y.-P. *Langmuir* **2003**, *19*, 7084.